

Release of Human TFIIB from Actively Transcribing Complexes Is Triggered upon Synthesis of 7- and 9-nt RNAs

Elina Ly[†], Abigail E. Powell^{†,‡}, James A. Goodrich and Jennifer F. Kugel

Department of Biochemistry, University of Colorado Boulder, 596 UCB, Boulder, CO 80309, USA

Correspondence to James A. Goodrich and Jennifer F. Kugel: james.goodrich@colorado.edu. jennifer. kugel@colorado.edu
https://doi.org/10.1016/j.jmb.2020.05.005
Edited by Achillefs Kapanidis

Abstract

RNA polymerase II (Pol II) and its general transcription factors assemble on the promoters of mRNA genes to form large macromolecular complexes that initiate transcription in a regulated manner. During early transcription, these complexes undergo dynamic rearrangement and disassembly as Pol II moves away from the start site of transcription and transitions into elongation. One step in disassembly is the release of the general transcription factor TFIIB, although the mechanism of release and its relationship to the activity of transcribing Pol II is not understood. We developed a single-molecule fluorescence transcription system to investigate TFIIB release *in vitro*. Leveraging our ability to distinguish active from inactive complexes, we found that nearly all transcriptionally active complexes release TFIIB during early transcription. Release is not dependent on the contacts TFIIB makes with its recognition element in promoter DNA. We identified two different points in early transcription at which release is triggered, reflecting heterogeneity across the population of actively transcribing complexes. TFIIB releases after both trigger points with similar kinetics, suggesting the rate of release is independent of the molecular transformations that prompt release. Together our data support the model that TFIIB release is important for Pol II to successfully escape the promoter as initiating complexes transition into elongation complexes.

© 2020 Elsevier Ltd. All rights reserved.

Introduction

Transcription by RNA polymerase II (Pol II) is a highly regulated process that involves interplay between Pol II, general transcription factors (GTFs), co-regulatory complexes, and gene-specific transcriptional activators and repressors [1-3]. The GTFs required to transcribe most protein-coding genes, TFIIA, TFIIB, TFIID, TFIIE, TFIIF, and TFIIH, assemble into preinitiation complexes (PIC) at the promoters of genes with Pol II and co-regulators such as Mediator [4–6]. GTFs play key roles in the formation of PICs, including binding core promoter elements in the DNA, recruitment and correct positioning of Pol II over the transcription start site, and stabilization of Pol II and other factors within PICs [1,7]. Biochemical, structural, and cellular studies have explored the mechanistic roles that each GTF embodies; however, much remains to be learned. This includes developing a better understanding of how GTFs release from complexes as they disassemble and Pol II moves away from the start site of transcription and transitions into elongation.

Toward this goal, we investigated the release of TFIIB from early transcribing complexes. TFIIB is a 33-kDa protein composed of several distinct structural domains that uniquely participate in different aspects of transcription. These include an N-terminal B ribbon region, a B reader domain, a B linker domain, and two cyclin-like repeat regions comprising the B core [8,9]. The B core regions directly interact with the TBP subunit of TFIID as well as the upstream core promoter element known as the TFIIB recognition element (BRE), which positions TFIIB on the DNA in the proper orientation for interactions with Pol II [10]. The B reader domain of TFIIB (composed of the B reader loop, B reader helix, and B reader strand regions) interacts directly with Pol II in a manner that could impact the release of TFIIB during early transcription. A crystal structure of TFIIB bound to

initially transcribing Pol II shows the B reader loop positioned in the RNA exit channel leading into the active site of Pol II [11]. A clash between the nascent RNA strand and the B reader loop is predicted to occur once the RNA reaches 7 nt in length, suggesting that TFIIB must undergo a conformational change or release its interactions with Pol II to accommodate the growing transcript [11]. Consistent with this, in vitro transcription assays have shown human TFIIB releases from the promoter DNA during transcription [12–15]; however, it could not be determined whether TFIIB specifically released from transcriptionally active complexes or dissociated from the bulk of inactive complexes in an unregulated manner. Indeed, extensive heterogeneity exists in reconstituted Pol II transcription complexes, and active complexes represent less than 20% of PICs [16-20]. Distinguishing whether TFIIB releases from active complexes or all complexes would suggest whether TFIIB release is an important mechanistic step during early transcription to allow Pol II to successfully transition into a processive elongation complex.

Here we determined the relationship between TFIIB release and active transcription complexes. We utilized a single-molecule transcription system that can uniquely identify active transcription complexes within a heterogeneous mix of active and inactive complexes [20]. We found that the vast majority of active transcription complexes released TFIIB in an NTP-dependent manner. This correlation and the rate of TFIIB release were not dependent on the interaction between TFIIB and the BRE, the core promoter element to which TFIIB binds. Furthermore, we identified two distinct points in early transcription at which release of TFIIB is triggered: during the addition of the seventh and ninth nucleotides to the growing RNA. The rates of TFIIB release after these trigger points are similar. Our data support a model that specific structural changes in transcribing complexes trigger TFIIB to release, then the protein dissociates over time as Pol II continues to transcribe. The strong correlation between the release of TFIIB and transcriptional activity leads us to propose that release of TFIIB from transcribing complexes is an important switch to release Pol II into a processive elongation complex.

Results and Discussion

Fluorescently labeled human TFIIB assembles into PICs and supports active transcription

To visualize TFIIB via single-molecule microscopy, we created a TFIIB construct containing a C-terminal SNAP tag to allow site-specific labeling with a fluorescent dye [21]. After expression and purifica-

tion, the TFIIB-SNAP protein was fluorescently labeled with an AlexaFluor488 SNAP dye substrate (AF488-TFIIB). The activity of AF488-TFIIB was compared to untagged TFIIB using a highly purified reconstituted human transcription system. Reactions contained Pol II, TBP, TFIIB, TFIIF, and a core promoter contained on a negatively supercoiled plasmid upstream of a G-less cassette that allowed an RNA product of defined length to be transcribed in the presence of ATP, CTP, and UTP. As shown in Figure 1(a), the fluorescent AF488-TFIIB had activity similar to that of the untagged protein, and the system was entirely dependent upon TFIIB.

We next included dye-labeled TFIIB in a fluorescence-based in vitro transcription assay that we previously developed [20]. For this assay, we labeled TFIIB-SNAP with AlexaFluor647 (AF647-TFIIB), which emits in the red channel. As diagrammed in Figure 1(b), this assay takes advantage of a three piece DNA construct containing a premelted bubble surrounding the transcription start site [22,23]. The template DNA strand has a Cy3 dye on its 5' end. The non-template DNA strand is composed of two separate oligonucleotides: 1) an upstream oligo that when annealed to the template strand creates the bubble from -9 to +3 due to mismatched bases, and 2) a downstream oligo that contains a BHQ2 quencher molecule on its 3' end that quenches emission from the Cy3 dye. After the addition of NTPs, Pol II transcribes the DNA and displaces the short nontemplate strand oligo, thereby revealing Cy3 emission. We chose take a reductionist approach and monitor the fate of TFIIB in a simplified system that used a pre-melted bubble, thereby eliminating the requirement for TFIIE and TFIIH to assist in promoter melting [22]. This approach has been applied to studies of other mechanistic transitions in early Pol II transcription [22-28]. Additional general factors can be added in the future to increase complexity and determine their unique roles in modulating the release of TFIIB.

We coupled this system with electrophoretic mobility shift assays to evaluate the assembly and activity of PICs containing untagged TFIIB or AF647-TFIIB. PICs were assembled on the three piece DNA construct, then half the reactions received NTPs lacking GTP. The first C residue in the template strand is at +35; hence, in the absence of GTP, Pol II pauses at +35 and remains bound to the promoter. All reactions were run in a native polyacrylamide gel (Figure 1(c)) that was scanned for Cy3 emission, the fluorophore on the DNA. The signal was very faint for unbound DNA (lanes 1-2) and for bound DNA without NTPs (lanes 3-4 and 7-8) due to the non-template strand guencher oligo. The addition of NTPs revealed Cy3 fluorescence (lanes 5-6 and 9-10), reflecting displacement of the quencher oligo due to transcription. This robust NTP-dependent increase in Cy3 emission was observed for PICs formed with either

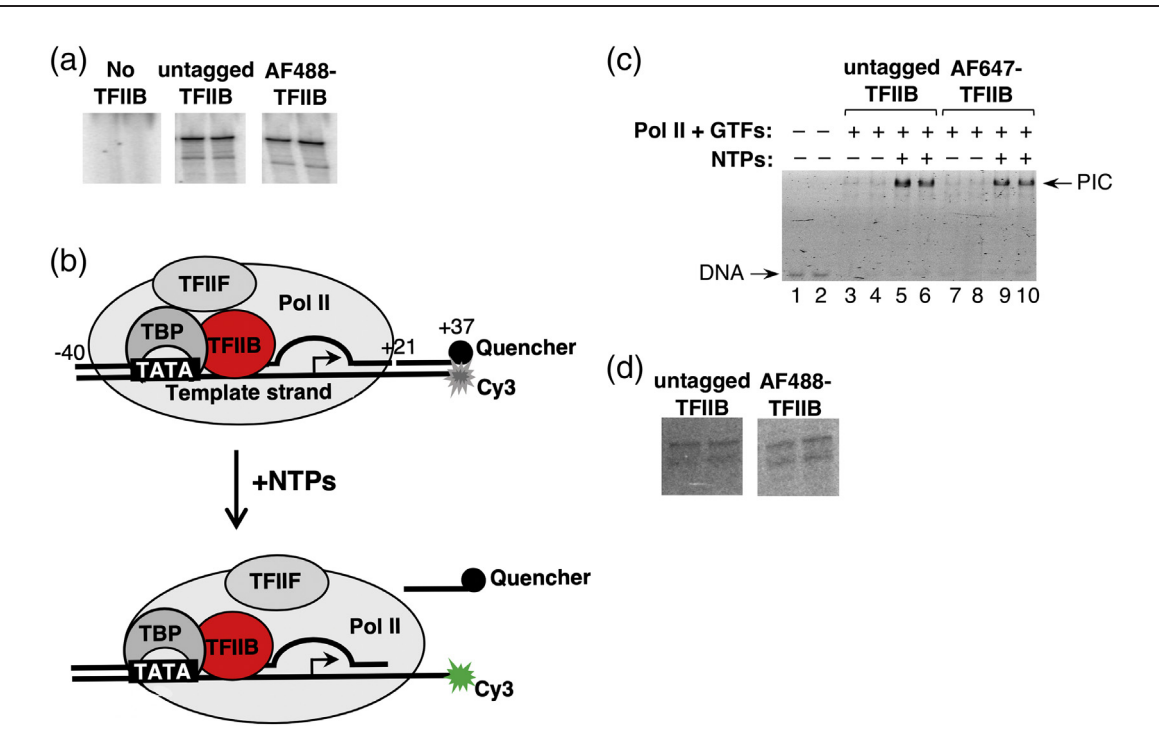


Figure 1. Fluorescent TFIIB-SNAP is active in Pol II transcription assays using a highly purified reconstituted human system. (a) Untagged TFIIB and AF488-TFIIB show similar activity in ensemble *in vitro* transcription reactions, and TFIIB is required. Shown are 390-nt G-less transcripts. Each condition was performed in replicate, and the data are from different regions of the same gel at the same exposure. (b) Schematic of the fluorescence-based transcription assay. PICs are assembled on a DNA construct containing a Cy3 fluorescent dye on the 5' end of the template strand that is quenched by a Black Hole Quencher 2 molecule attached to a short oligo. After the addition of NTPs, the quencher oligo is displaced by transcribing Pol II, resulting in the appearance of Cy3 fluorescence. Fluorescent AF647-TFIIB is shown in red. (c) AF647-TFIIB supports PIC formation and active transcription in the quencher-release assay. Transcription complexes were resolved using an electrophoretic mobility shift assay, and the gel was scanned for Cy3 emission. Reactions contained the quenched DNA construct only (lanes 1–2) or PICs formed with either TFIIB (lanes 3–6) or AF647-TFIIB (7–10). NTPs were added to reactions resolved in lanes 5–6 and 9–10. (d) Similar levels of transcripts are produced from the three piece DNA template with untagged TFIIB or AF488-TFIIB. Shown are RNA transcripts from replicate reactions, and data are from different regions of the same gel at the same exposure. The lower band is 35 nt in length, and we believe the upper band is 2–3 nt longer due to transcript slipping, but has the same 3' end [24,38].

untagged TFIIB or AF647-TFIIB. In addition, similar levels of RNA transcripts were produced from the three piece DNA construct in reactions containing untagged TFIIB or fluorescent TFIIB (Figure 1(d)).

Nearly all active transcription complexes release TFIIB

We next investigated the relationship between active transcription complexes and the release of TFIIB by using AF647-TFIIB and the quencher release assay in single-molecule experiments. Prior single-molecule studies with the quencher-release assay showed that transcriptional activity required the presence of all three GTFs and Pol II, and that ~10%–20% of complexes were active [20]. As diagrammed in Figure 2(a), the three-piece DNA construct was immobilized on the surface of a streptavidin-derivatized slide using a 5' biotin on the long non-template strand oligo. This system can resolve active from inactive transcription complexes

by identifying individual PICs that contained AF647-TFIIB and also released the quencher oligo after the addition of NTPs. To do so, images of surface immobilized Cy3-DNA (green) and AF647-TFIIB (red) molecules before and after the addition of NTPs were collected using a total internal reflection fluorescence (TIRF) microscope. Co-localization of red spots on the surface prior to NTPs (i.e. PICs containing AF647-TFIIB) with green spots on the surface after NTPs (i.e. quencher oligo was released) allowed us to identify individual transcription complexes that were active. After identifying active complexes, we inquired about the fate of TFIIB.

As a control to test the robustness of the red and green co-localization in our system, we first assembled PICs containing AF647-TFIIB on promoter DNA that lacked the quencher oligo so Cy3 emission could be observed in the absence of NTPs. Images of red and green emission were obtained with a TIRF microscope, and single PICs were identified using co-localization. We found that 34% of the Cy3-DNA

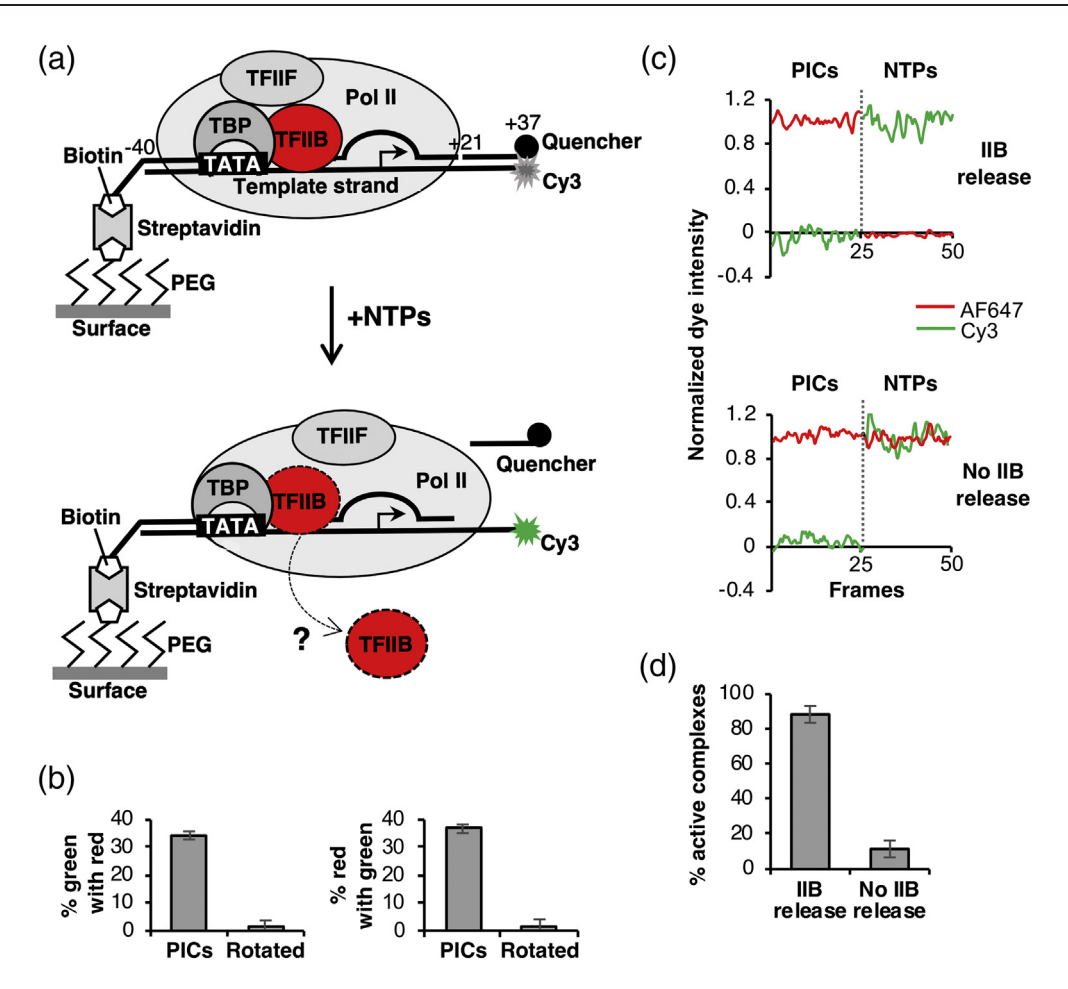


Figure 2. TFIIB releases from nearly all transcriptionally active complexes. (a) Schematic of the single-molecule transcription assay. PICs are immobilized on slides through a biotin on the long non-template strand oligo that binds a streptavidin-derivatized slide surface. The quencher oligo is displaced by transcribing Pol II, resulting in the appearance of Cy3 fluorescence. The fate of AF647-TFIIB in the active complexes can be determined from emission in the red channel. (b) Single-molecule co-localization of AF647-TFIIB emission and Cy3-DNA emission is highly specific. Plotted are AF647 (red) and Cy3 (green) co-localized spots in PICs and after one image was rotated 90°. Each bar is the average of four regions, and the errors are the standard deviations. (c) Single-molecule intensity traces of Cy3 and AF647 emission from co-localized green/red spot pairs were used to determine the fate of AF647-TFIIB in active transcription complexes after the addition of NTPs. Shown are representative traces from active complexes that either released TFIIB (top) or retained TFIIB (bottom). To create the plots, 25 frames of PIC emission were merged with 25 frames of emission after NTPs. (d) The majority of transcriptionally active complexes release TFIIB after addition of NTPs. Data are from 248 co-localized spot pairs representing active complexes. Plotted is the average of four regions, and the errors are the standard deviations.

spots (green) co-localized with AF647-TFIIB spots (red), and 36% of the AF647-TFIIB spots co-localized with Cy3-DNA spots (Figure 2(b)). Importantly, when Cy3 emission images were rotated 90°, only 1%–2% co-localization of green and red spot pairs was observed, demonstrating that random co-localization in this system is negligible.

Using this single-molecule system, we asked whether there was a relationship between the activity of a transcription complex and whether TFIIB released from the DNA after the addition of NTPs. PICs containing AF647-TFIIB were immobilized on the surface of a slide, and Cy3 (green) and AF647 (red) emission movies were collected with a

TIRF microscope. NTPs were added for 5 min, and a second set of Cy3 and AF647 emission movies was collected over the same regions. We identified the individual PICs that contained AF647-TFIIB prior to the addition of NTPs (i.e. red spots on the slide) and were also transcriptionally active upon NTP addition (i.e. green spots after the addition of NTPs that colocalized with red spots prior to NTPs). We then determined whether TFIIB released from each active PIC by evaluating whether AF647 emission was lost after the addition of NTPs.

Figure 2(c) shows emission data from two different active complexes. On the top, a loss of AF647 intensity (red) was observed after the addition of

NTPs, indicating that AF647-TFIIB released from this complex during transcription. The NTPdependent increase in Cy3 signal (green) showed the complex was transcriptionally active. For comparison, the data on the bottom of Figure 2(c) were obtained from a complex that was transcriptionally active but did not release AF647-TFIIB during transcription. Here, the Cy3 emission increased with NTP addition; however, the AF647 emission did not change. This analysis was performed for 248 transcriptionally active complexes. As shown in Figure 2(d), 88.5% of active complexes released AF647-TFIIB, while only 11.5% retained AF647-TFIIB. To estimate the level of TFIIB release from transcriptionally inactive complexes, we monitored spots of AF647 intensity at which a green dye did not appear upon the addition of NTPs. Importantly, there was not an NTP-dependent increase in AF647-TFIIB released from these transcriptionally inactive spots.

We also considered whether photobleaching of the AF647 dye would impact our analysis of TFIIB release after NTP addition. To minimize the chance of mis-interpreting photobleaching as TFIIB release, slides were only imaged for 12.5 s (25 frames with a 0.5-s frame rate) at a fairly low laser power before and after NTP addition. To directly evaluate photobleaching, we re-analyzed 220 active complexes that showed NTP-dependent TFIIB release. We looked at the 25 frames of red emission data that were taken after the 5-min incubation with NTPs when the laser was off; these complexes showed red TFIIB emission prior to the addition of NTPs. Only two complexes showed loss of red emission during the time the laser was on, and 218 of the active complexes lost their red signal (i.e. TFIIB released) during the NTP incubation when the laser was off. Therefore, loss of red signal could potentially be due to photobleaching less than 1% of the time.

Here we uniquely show that the NTP-dependent release of TFIIB is tightly correlated with transcriptional activity. By making this connection, our singlemolecule data lead us to propose that release of TFIIB is an important structural re-arrangement that helps maintain Pol II activity as elongation complexes form. In other words, release of TFIIB is critical for Pol II to escape the promoter and transition into a processive elongation complex. This model was first suggested several years ago when the co-crystal structure of an initially transcribing Pol II and TFIIB showed that the nascent RNA would likely clash with TFIIB during early transcription [11]. The strong correlation we observed here provides functional evidence in support of this structural model. Moreover, it is possible that failure to undergo the proper structural transformations that trigger TFIIB release could contribute to the high fraction of inactive complexes observed in vitro. Although our data show a strong correlation between TFIIB release and the transcriptional activity of Pol II,

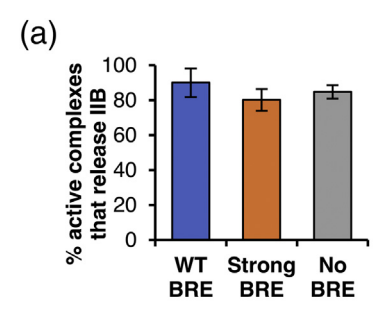
they do not directly show cause and effect. It is possible a mutant TFIIB with impaired release could more fully test causation. Studies have identified mutations in the B reader region that do not impact the ability of TFIIB to assemble into complexes [14,29]. Perhaps mutations in the B reader could be used to test whether TFIIB release indeed is required for Pol II to escape the promoter and transition into a processive elongation complex.

Although the vast majority of active complexes released TFIIB, we observed a small fraction of active complexes (~11%) that retained TFIIB. Interestingly, studies of *Escherichia coli* transcription have shown that the σ^{70} subunit of the polymerase predominantly releases from active transcription complexes; however, it is retained about 30% of the time and might play a regulatory role in transcriptional elongation [30]. There is structural homology between the B reader loop and the 3.2 loop region of σ^{70} [31]. Therefore, it is plausible that retention of TFIIB in a small population of active complexes is a part of an unrecognized regulatory mechanism.

The rate of TFIIB release from active complexes suggests a trigger mechanism that is not impacted by the BRE

TFIIB can contact the DNA at an upstream core promoter element known as the BRE, which helps position TFIIB in the proper orientation for interaction with Pol II [10]. Accordingly, we asked whether the BRE sequence might influence the relationship between TFIIB release and active transcription. The BRE sequence in our DNA construct is from the adenovirus major late promoter (AdMLP) and differs from consensus at two positions. We made two additional DNA constructs in which the AdMLP BRE was either mutated to a perfect consensus sequence (strong BRE) or a completely non-consensus sequence (No BRE). Single-molecule transcription assays were performed with the three DNAs to determine the percentage of active complexes that released TFIIB. We found no significant difference between the three promoters (Figure 3(a)). Hence, the BRE does not influence the tight correlation between active transcription and TFIIB release.

These data suggest that whatever the role the BRE plays in positioning TFIIB in PICs, it does so in a manner that does not directly impact the release of TFIIB from active complexes. In other words, the protein–protein or protein–nucleic acid contacts that must be rearranged to allow TFIIB to release are not controlled by the BRE. The BRE does, however, play a positive role in transcription. Biochemical experiments have shown that the BRE enhances transcription levels [10]. Consistent with this, in our single-molecule experiments, the number of active complexes was ~30% higher on the strong BRE compared to the No BRE template, suggesting that



(b)

Rate of IIB release from active complexes

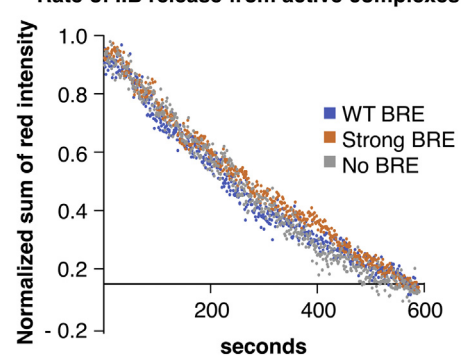


Figure 3. The extent and rate of TFIIB release are not controlled by the BRE. (a) The percentage of active complexes that released TFIIB was similar with a wild-type BRE, a strong BRE, or no BRE; there were 209, 441, and 300 active complexes included in each analysis, respectively. Plotted are the averages of four regions, and the errors are the standard deviations. (b) The rate at which TFIIB releases from active complexes is independent of the BRE. For each promoter, normalized, summed AF647 emission data are plotted as the average of two replicates. There were 91, 62, and 81 active complexes included in the WT, strong, and no BRE analyses, respectively.

the BRE facilitates the formation of active complexes but not the release of TFIIB during transcription.

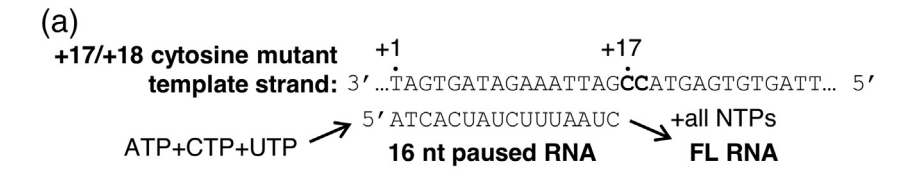
We next asked whether the BRE impacts the rate at which TFIIB releases from complexes during early transcription. We performed single-molecule transcription assays on either the wild-type promoter (WT), the strong BRE promoter, or the No BRE promoter. After flowing NTPs over the slide to initiate transcription, AF647 emission was recorded for 10 min to monitor AF647-TFIIB release in real time. Then a short Cv3 emission movie was recorded to identify the DNAs that were transcribed, enabling us to mark the positions of active complexes on the slide surface. We analyzed the data to identify the active transcription complexes that released AF647-TFIIB after NTPs were added. For these complexes, the fluorescence intensity values at each frame of the 10-min movie were normalized to the maximum intensity, then summed for all

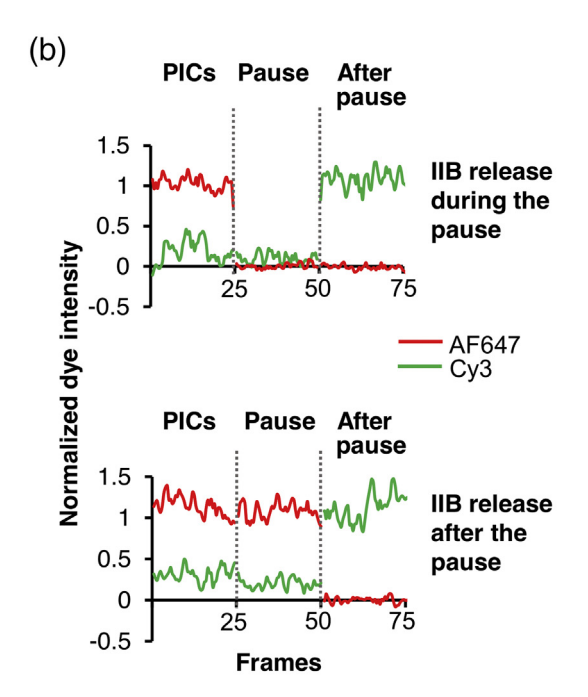
complexes in two replicates. The data for the three promoters were normalized to 1.0 and plotted *versus* time to generate a kinetic view of AF647-TFIIB release (Figure 3(b)). The half-time for release at each of the three promoters was ~5 min, showing that the BRE does not significantly impact the rate of TFIIB release. As a control, we measured the rate at which AF647-TFIIB dissociated from PICs in the absence of NTPs. The half-time was ~12 min, which is longer than the half-times for NTP-triggered AF647-TFIIB release, and more similar to measurements of PIC decay rates [32]. Therefore, the TFIIB release we observed was NTP-dependent.

Finding that the BRE also did not impact the rate of release underscores the conclusion that the molecular interactions controlled by the BRE do not regulate TFIIB release. It is most likely that TFIIB makes multifaceted interactions with PIC components; therefore, a network of structural changes is required to enable release. Consistent with this, we found that the kinetic data in Figure 3(b) did not fit well with either a single or double exponential equation, suggesting a multi-step mechanism of release. The rate of TFIIB release we measured is slower than the rate of transcription we previously measured on this promoter using ensemble transcription experiments [33]. This suggests a model in which the release of TFIIB is triggered by an event(s) during early RNA synthesis, then once triggered TFIIB dissociates from complexes at a defined rate as Pol II continues to rapidly transcribe. Interestingly, archaeal transcription factor B (TFB), the homolog of TFIIB, exhibits a multi-step mechanism of release in which the TFB reader domain undergoes structural transformations within complexes between registers +6 and + 10, then TFB release is detected at +15 and beyond [34]. It is possible an analogous multi-step mechanism occurs with human TFIIB. Assays that detect conformational changes within active transcription complexes will be required to decipher the structural changes that trigger release of TFIIB.

TFIIB release is triggered during synthesis of 7and 9-nt RNAs

We next asked whether TFIIB release is triggered at a distinct point or heterogeneously during early transcription. To do so we forced Pol II to pause at specific positions in the early transcribed region using a series of DNAs that each contained a double cytosine mutation in the transcribed region of the template strand. For example, Figure 4(a) shows the sequence of the template strand of the DNA with cytosines at positions +17 and + 18. When ATP, CTP, and UTP were flowed onto the surface of a slide containing PICs assembled on this DNA, Pol II paused after synthesis of a 16-nt RNA due to the lack of GTP. By subsequently flowing in a complete set of nucleotides, Pol II was freed from the pause, elongated the 16-nt RNA to full-





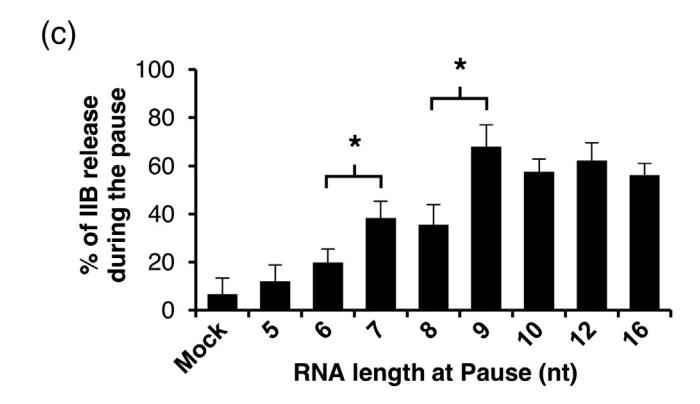


Figure 4. TFIIB release occurs at two distinct points during early transcription. (a) Cytosine mutant DNA constructs contained two sequential cytosines at various DNA positions on the template strand oligo. The +17/+18 cytosine mutant DNA is shown. On this template, the addition of ATP, CTP, and UTP allows formation of a stable paused complex containing a 16-nt RNA that can be elongated after addition of all NTPs. (b) Shown are representative intensity traces of Cy3 and AF647 emission for single complexes assembled on the cytosine mutant DNA that allowed Pol II to pause after synthesis of a 7-nt RNA. The data on top revealed that AF647-TFIIB released during the pause, whereas the data on the bottom revealed that AF647-TFIIB released after Pol II was freed from the pause. To create the plots, 25 frames of emission data from each stage of the reaction were merged. (c) TFIIB release is triggered after synthesis of a 7-nt RNA and a 9-nt RNA. The percentage of transcriptionally active complexes that released AF647-TFIIB during the pause was plotted. Data are the average of eight regions, and the errors are the standard deviations. The asterisks indicate where neighboring bars are statistically different (p < 0.01, unpaired two-tailed *t-test*). The p values from the *t-test*s comparing the neighboring bars are as follows: 5 nt *versus* 6 nt, p = 0.03; 6 nt *versus* 7 nt, p = 0.00005; 7 nt *versus* 8 nt, p = 0.5; 8 nt *versus* 9 nt, p = 0.000003; 9 nt *versus* 10 nt, p = 0.01; 10 nt *versus* 12 nt, p = 0.2; 12 nt *versus* 16 nt, p = 0.07. The following numbers of active complexes were analyzed, listed according to the RNA length at the pause: 5 nt, 230; 6 nt, 351; 7 nt, 1160; 8 nt, 1482; 9 nt, 655; 10 nt, 127; 12 nt, 258; 16 nt, 401.

length RNA, and displaced the quencher oligo. Pause and release experiments such as these have been widely used to dissect mechanistic steps in Pol II transcription. Using this approach, transcription was paused at eight different positions during early transcription. For each DNA template, we sequentially collected three sets of Cy3 and AF647 emission movies from the same regions of a slide in the following order: 1) PICs on the surface prior to the addition of NTPs; 2) paused complexes after a 2.5-min incubation with ATP, UTP, and CTP; and 3) complexes after a 5-min incubation with the full set of NTPs. The lasers were only turned on during the short 12.5-s imaging window after each step to minimize photobleaching as a consideration.

Using these emission movies, we first identified spot pairs that showed active transcription and TFIIB release. We then determined whether AF647-TFIIB released during the pause or after Pol II was freed from the pause. Examples of each outcome are shown in the emission traces for two spot pairs (Figure 4(b)) from complexes assembled on the +8/+9 cytosine mutant template (7-nt paused RNA). In the upper panel, AF647-TFIIB released during the pause (i.e. loss of AF647 emission after frame 25 and prior to frame 50). In the lower panel, AF647-TFIIB released after Pol II was freed from the pause (i.e. loss of AF647 emission after frame 50). For each of the eight DNA templates that paused Pol II at a different point during early transcription, we identified the active complexes that showed AF647-TFIIB release, then calculated the percentage that released during the pause (Figure 4 (c)). We performed unpaired two-tailed *t-test*s to compare the percentage of TFIIB released with each nucleotide addition to the paused RNA. There were two transitions that showed strong statistical significance for the increase in active complexes that released TFIIB: during synthesis of a 7-nt RNA and a 9-nt RNA. The p values for these transitions were <0.0001 and orders of magnitude lower than the p values for all other transitions. Hence, the data support the model that release of AF647-TFIIB from active transcription complexes is triggered predominantly with synthesis of a 7-nt RNA and a 9-nt RNA. Prior to synthesis of a 7-nt RNA, a low constant level of release was observed, and after synthesis of a 9-nt RNA, the level of release plateaued.

Our data show that there are two prominent points at which TFIIB release is triggered during early transcription. This reflects heterogeneity even within the population of active complexes, which would not have been possible to resolve using ensemble experiments. Although we believe our statistical analyses support two distinct trigger points for release, it remains possible that heterogeneity between complexes could lead to TFIIB release taking place probabilistically and at slightly different positions each time. We favor a model in which TFIIB release is triggered by distinct conformational changes within

transcribing complexes that occur with synthesis of 7and 9-nt RNAs that serve to destabilize TFIIB contacts with Pol II, and perhaps other GTFs. The first of these conformational changes likely involves removing the TFIIB reader loop from the RNA exit channel of Pol II. as predicted by structural data [11]. Ensemble biochemical experiments have also suggested that destabilization of TFIIB within complexes occurs upon synthesis of a 7-nt RNA [15]. It is less clear what conformational transformations coincide with synthesis of a 9-nt RNA. In addition to breaking contacts between TFIIB and Pol II, these transformations could involve TFIIF, since data show that interactions with TFIIF are critical for holding TFIIB within complexes during initiation [15]. Ensemble biochemical experiments found TFIIB release occurring between synthesis of 10- and 13-nt RNAs [15]. The differences with our findings could be attributable to the single-molecule assays detecting release exclusively from active complexes. Inactive complexes are the vast majority (~80-90%) and are likely heterogenous in their decay and the points in transcription at which they become inactive, making it possible to observe different outcomes between the two experimental systems.

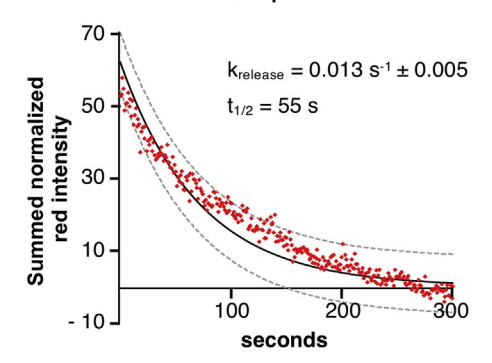
TFIIB release dissociates from the two populations of complexes with a similar rate

To potentially identify unique characteristics of TFIIB release after the two trigger points, we measured the subsequent rates of release. To do so, we paused transcription after synthesis of a 6-nt RNA or an 8-nt RNA, just prior to the trigger points for release, and recorded short Cv3 and AF647 emission movies to mark the positions of complexes on the surface. The complete set of nucleotides was then flowed in to free the paused Pol II, and AF647 emission was recorded for 5 min to monitor AF647-TFIIB release in real time. Lastly, a short Cy3 emission movie was recorded to identify the DNAs that were transcribed. We analyzed the data to identify active transcription complexes that released AF647-TFIIB after Pol II was freed from the pause. For these complexes, the fluorescence intensity values at each frame of the 5-min movie were normalized to the maximum intensity value, then data for all complexes were summed, plotted, and fit to a single exponential (Figure 5). The average k_{release} values for AF647-TFIIB after freeing Pol II from the 6-nt pause and the 8nt pause were not substantially different from one another $(0.013 \pm 0.005 \text{ s}^{-1})$ and $0.014 \pm 0.002 \text{ s}^{-1}$, respectively); the half-times for release are ~52 s.

The populations of complexes that release TFIIB after synthesis of a 7- or 9-nt RNA are kinetically indistinguishable. Therefore, the rate at which TFIIB releases from transcribing complexes is not dependent on the different molecular transformations that trigger its release at the two unique positions. This is consistent with our model that specific structural

changes allow, or trigger, TFIIB to release; then TFIIB dissociates with a defined rate as Pol II continues to transcribe the template. This is in contrast to a model in which the polymerase pauses at the trigger points and only continues transcribing after TFIIB release occurs. Interestingly, the rates of TFIIB release we measured after freeing Pol II from paused complexes (Figure 5) are faster than the rate of TFIIB release we measured after the initial addition of NTPs (Figure 3 (b)). This suggests that a kinetically slow step occurs prior to or coincident with synthesis of a 6-nt RNA (the first pause point). The slow step could involve a structural transformation that occurs early after initiation that impacts the positioning of TFIIB in

${\rm (a)}_{ m Rate}$ of IIB release after pause with 6 nt RNA



(b) Rate of IIB release after pause with 8 nt RNA

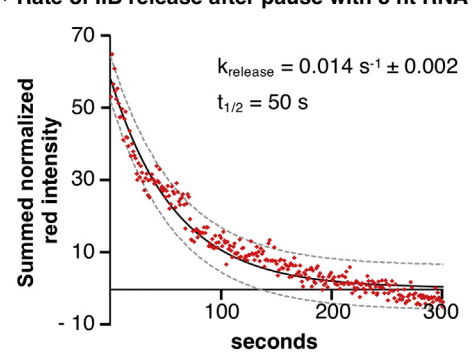


Figure 5. TFIIB releases with a similar rate after the two trigger points in early transcription. Pol II was paused after synthesis of a 6-nt RNA (top plot) or an 8-nt RNA (bottom plot), then the rate of AF647-TFIIB release was measured as Pol II was freed from each pause. Normalized, summed AF647 emission data (red points) over time were plotted and fit with a single exponential (black lines); the dashed lines represent the 95% confidence intervals of the fits. The average $k_{\rm release}$ values after Pol II was freed from the pauses are shown. The rate constants are the average of two measurements, and the errors are the ranges in the data. The $t_{\rm 1/2}$ values were calculated from the average $k_{\rm release}$ values. 96 and 127 active complexes were included in the rate measurements for the 6- and 8-nt paused RNAs, respectively.

complexes. Our data do not reveal the nature of this transformation, but it could include changes to the network of protein-protein contacts, protein-promoter contacts, or the RNA-DNA hybrid. Because we performed these experiments using a template with a mismatched region to form the bubble, transcribing complexes could not undergo bubble collapse. This transition occurs after the melted region grows to ~18 unpaired bases at which point the upstream edge of the transcription bubble collapses and re-anneals. Prior studies have shown that bubble collapse occurs once the nascent transcript is at least 7 nt in length [35]. This is similar to the points at which we observe triggering of TFIIB release; hence, it is possible that the rate with which TFIIB releases and/or the positions of the trigger points could be impacted by the structural rearrangements that occur when the upstream edge of the bubble collapses. Indeed, a relationship between bubble collapse, Pol II pausing at +7 to +9, and the presence of TFIIB within Pol II have been proposed [35].

Using our single-molecule transcription system to resolve active from inactive complexes revealed the tight correlation between transcriptional activity and release of TFIIB. Moreover, we discovered heterogeneity within active complexes that is marked by two different trigger points for TFIIB release during early transcription. We are now positioned to label other GTFs to study additional mechanisms by which active PICs disassemble as Pol II transitions into elongation.

Materials and Methods

Cloning, expression, purification, and labeling of TFIIB-SNAP

The TFIIB-SNAP construct contained TFIIB followed by an 8-amino-acid linker (GSSGGSSG), a SNAP tag, and a His tag. DNAs encoding TFIIB and SNAP were amplified using PCR and inserted into a pET21a + expression vector using Ndel and BamHI restriction sites. TFIIB-SNAP was expressed in BL21 E. coli cells. The cell pellet was lysed by sonication in Buffer A (20 mM Tris (pH 7.9), 500 mM NaCl, 10% glycerol, 2 mM DTT, 0.5 mM PMSF, and 1× EDTAfree Protease Inhibitor (Roche)) and centrifuged. The supernatant was loaded on a HisPur Ni-NTA (Thermo Scientific) column pre-equilibrated with Buffer A. The column was washed multiple times with Buffer A followed by Buffer A containing 50 mM imidazole. TFIIB-SNAP was eluted with Buffer A containing 300 mM imidazole. The eluate was dialyzed overnight at 4 °C into 10 mM Tris (pH 7.9), 50 mM KCl, 1 mM DTT, and 10% glycerol. To fluorescently label the protein, 100 µl of 2 µM TFIIB-SNAP was incubated with 10 µM SNAP-Surface AlexaFluor dye substrate (New England Biolabs) for 2 h at room temperature in

the dark. Excess free dye was removed using Zeba Spin Desalting columns (7 K MWCO, 0.5 ml, Thermo Scientific).

Three piece DNA constructs for fluorescent transcription assays

The DNA contained the AdMLP from -40 to -1 and a downstream sequence optimized for template usage, as previously described [20]. Constructs were generated by annealing three oligos (the BRE is underlined and the start site is in bold): 1) template strand oligo (-40 to +37) containing a 3' Cy3 fluorophore: 5'CCTGAGGTTAGTGTGAGTAGTGAT-TAAAGATAGTGATGAGGACGAACGCGCCCC-CACCCCTTTTATAGCCCCCCTT3', 2) long nontemplate strand oligo (-40 to +20): 5'AAGGGGGGC-TATAAAAGGGGGTGGGGGCGCGAAGCAGGAG-TAGACTATCTTTAATCACTA3', and 3) short nontemplate strand oligo (+21 to +37) containing a 3' BHQ2 quencher: 5'CTCACACTAACCTCAGG3'. The first C residue in the template strand is at +35; hence, in the absence of GTP, Pol II pauses at +35. The sequence of the non-template and template strands from -9 to +3 will not anneal in order to create a premelted region. For single-molecule experiments, the long non-template strand oligo contained 5'-biotin-TACGAGGAAT to enable surface immobilization. For the BRE mutants, the AdMLP BRE sequence (GGGGGC, non-template strand underlined above) was changed to GGGCGCC and AACTCGG for the strong BRE and No BRE, respectively. For pausing experiments, the following DNA positions were individually mutated to CC on the template strand and GG on the non-template strand: +7/+8. +8/+9. +9/+10. +10/+11, +11/+12, +13/+14, +17/+18. All oligos except the short non-template strand oligo were gel purified prior to annealing. In annealing reactions, the molar ratio of template oligo:long non-template oligo: short non-template oligo was 2:1:10. The oligos were annealed in a thermocycler as follows: 5 min at 95 °C, cool to 60 °C at 0.1 °C per second, 1 h at 60 °C, cool to 45 °C at 0.1 °C per second, 1 h at 45 °C, cool to 4 ° C at 0.1 °C per second.

Ensemble transcription assays

Recombinant human TBP, untagged TFIIB, TFIIF, and native human Pol II were prepared as described previously [20]. The ensemble *in vitro* transcription reactions were assembled as previously described [20]. Briefly, reactions were performed in 10% glycerol, 10 mM Tris (pH 7.9), 50 mM KCI, 1 mM DTT, 0.05 mg/ml BSA, 10 mM Hepes (pH 7.9), and 4 mM MgCl₂. Reactions contained 1–2 nM DNA, either the three piece construct or plasmid DNA containing the AdMLP fused to a 390-bp G-less cassette [36]. Proteins were added to the reactions at final concentrations of 3.5 nM TBP, 2 nM TFIIF, 2 nM Pol II, and

10 nM untagged TFIIB or fluorescently labeled TFIIB-SNAP. PICs were formed by incubation for 20 min at room temperature, then NTPs were added for 20 min (625 μ M ATP, UTP, and 25 μ M [32 P]CTP, 5 Ci per reaction). Reactions were stopped and RNA transcripts were ethanol precipitated as described [16]. The RNA was resolved in 6% (Figure 1(a)) or 20% (Figure 1(d)) denaturing gels. To observe the formation of PICs and quencher oligo release (Figure 1(c)), reactions were run on 4% native gels containing 0.5X TBE and 5% glycerol [20]. Native gels were imaged by scanning with a 532-nm laser and reading fluorescence emission using a 580-nm emission filter on a Typhoon Imager 9400 (GE biosciences).

Single-molecule transcription assays

The cleaning and assembly of the flow chambers, the surface functionalization, and the preparation of streptavidin, D-glucose, glucose oxidase, catalase, and 100 mM Trolox stock solutions were as previously described [37]. PICs were formed by incubating 0.15-0.25 nM biotinylated three piece DNA with 3.5 nM TBP, 5 nM AF647-TFIIB, 2 nM TFIIF, 2-3 nM Pol II, and 0.5 ng/µl poly(dG:dC) competitor DNA in DB/RM buffer (10 mM Tris (pH 7.9), 10 mM Hepes (pH 7.9), 50 mM KCl, 4 mM MgCl₂, 10% glycerol, 1 mM DTT, 0.1 mg/ml BSA) for 20 min at room temperature. PICs were then flowed onto the surface and incubated for 10 min. The surface was washed twice with DB/RM buffer, then Imaging Buffer (1.02 mg/ml glucose oxidase, 0.04 mg/ml catalase, 0.83% D-glucose, and 3.45 mM Trolox in DB/RM buffer) was flowed into slide chambers. For non-pausing transcription assays, NTPs (625 µM ATP, CTP, and UTP) diluted in Imaging Buffer were flowed into slide chambers and incubated for 5 min. For pausing assays, all NTP solutions were made in Imaging Buffer containing 1.6 U/µl of Murine RNase Inhibitor (New England Biolabs). To pause after synthesis of a 5-nt RNA, PICs were assembled on wild-type DNA and 1 mM ApU, 625 µM ATP, and 625 µM CTP were added for 2.5 min. To pause transcription at other positions, PICs were assembled on cytosine mutant DNAs and 625 µM ATP, CTP, and UTP were added for 2.5 min. For the mock pause control, a solution lacking NTPs was used. In all cases, the pause was released by incubation with a solution of 625 µM ATP, CTP, UTP, and GTP for 5 min.

Single-molecule data collection and analysis

Flow chambers were imaged using an objective based TIRF microscope (Nikon TE-2000 U) equipped with a 1.49 NA immersion objective, a Piezo nanopositioning stage, and two CCD cameras. Samples were excited with 532 nm (green) and 635 nm (red) continuous wave lasers, and emission images were collected by an Evolve Photometric CCD and a Cascade II Photometric CCD, respectively.

Green and red emission movies were sequentially recorded using the NIS-elements software at 0.5-s exposure time for 25 frames, except for the kinetic experiments, which used a 1-s exposure time over the time frames noted in Results and Discussion. By using the Piezo nanopositioning stage, green and red emission movies across the same regions were recorded for PICs and after NTP addition. These movies were analyzed with in-house co-localization software to identify green/red spot pairs representing quencher released from PICs with AF647-TFIIB. As a control, co-localization analyses were also performed with the Cy3 image rotated by 90° to ensure that colocalization was not due to random overlap of spots. Fluorescence emission traces for every co-localized spot pair were individually viewed and analyzed. The green intensity traces for each spot pair were used to identify active transcription complexes *via* an increase in Cy3 emission due to guencher release after the addition of NTPs. The red intensity traces for each spot pair were used to determine if and when TFIIB released from Pol II via a decrease in AF647 emission.

Acknowledgments

This work was supported by the National Science Foundation (MCB-1817442 and DGE1144083 to E. L.) and the National Institutes of Health (T32 GM08759 to E.L. and T32 GM065103 to A.E.P).

Author Contributions

Conceptualization: E.L., A.E.P., J.A.G., J.F.K.; reagent preparation and single-molecule data collection: E.L., A.E.P.; data analyses: E.L., A.E.P., J.A. G., J.F.K.; funding acquisition: E.L., J.A.G., J.F.K.; software: J.A.G.; supervision: J.A.G., J.F.K.; writing: E.L., J.A.G., J.F.K. All authors edited and approved the final manuscript.

Received 19 December 2019; Received in revised form 8 May 2020; Accepted 11 May 2020 Available online 14 May 2020

Keywords:

transcription; single molecule; general transcription factor; RNA polymerase II; TIRF

E.L. and A.E.P. contributed equally to this work.

‡Present address: A.E. Powell, Department of Biochem-

istry, School of Medicine, Stanford University, Stanford, CA 94305, USA.

Abbreviations used:

Pol II, RNA polymerase II; GTF, general transcription factor; TFII, transcription factor of Pol II; PIC, preinitiation complex; AF488-TFIIB, TFIIB labeled with AlexaFluor488; AF647-TFIIB, TFIIB labeled with AlexaFluor647; BRE, TFIIB recognition element; TIRF, total internal reflection fluorescence; AdMLP, adenovirus major late promoter.

References

- [1] Thomas, M.C., Chiang, C.M., (2006). The general transcription machinery and general cofactors. *Crit. Rev. Biochem. Mol. Biol.*, 41, 105–178.
- [2] Kadonaga, J.T., (2004). Regulation of RNA polymerase II transcription by sequence-specific DNA binding factors. Cell, 116. 247–257.
- [3] Krasnov, A.N., Mazina, M.Y., Nikolenko, J.V., Vorobyeva, N. E., (2016). On the way of revealing coactivator complexes cross-talk during transcriptional activation. *Cell. Biosci.*, 6, 1–15
- [4] He, Y., Fang, J., Taatjes, D.J., Nogales, E., (2013). Structural visualization of key steps in human transcription initiation. *Nature*, 495, 481–486.
- [5] Murakami, K., Elmlund, H., Kalisman, N., Bushnell, D.A., Adams, C.M., Azubel, M., Elmlund, D., Levi-Kalisman, Y., et al., (2013). Architecture of an RNA polymerase II transcription pre-initiation complex. *Science*, 342, 1238724.
- [6] Schilbach, S., Hantsche, M., Tegunov, D., Dienemann, C., Wigge, C., Urlaub, H., Cramer, P., (2017). Structures of transcription pre-initiation complex with TFIIH and Mediator. *Nature*, 551, 204–209.
- [7] Sainsbury, S., Bernecky, C., Cramer, P., (2015). Structural basis of transcription initiation by RNA polymerase II. *Nat. Rev. Mol. Cell Biol.*, 16, 129–143.
- [8] Buratowski, S., Zhou, H., (1993). Functional domains of transcription factor TFIIB. *Proc. Natl. Acad. Sci. U. S. A.*, 90, 5633–5637.
- [9] Bushnell, D.A., Westover, K.D., Davis, R.E., Kornberg, R. D., (2004). Structural basis of transcription: an RNA polymerase II-TFIIB cocrystal at 4.5 angstroms. *Science*, 303, 983–988.
- [10] Lagrange, T., Kapanidis, A.N., Tang, H., Reinberg, D., Ebright, R.H., (1998). New core promoter element in RNA polymerase II-dependent transcription: sequence-specific DNA binding by transcription factor IIB. *Genes Dev.*, 12, 34–44.
- [11] Sainsbury, S., Niesser, J., Cramer, P., (2013). Structure and function of the initially transcribing RNA polymerase II-TFIIB complex. *Nature*, 493, 437–440.
- [12] Yudkovsky, N., Ranish, J.A., Hahn, S., (2000). A transcription reinitiation intermediate that is stabilized by activator. *Nature*, 408, 225–229.
- [13] Zawel, L., Kumar, K.P., Reinberg, D., (1995). Recycling of the general transcription factors during RNA polymerase II transcription. *Genes Dev.*, 9, 1479–1490.
- [14] Tran, K., Gralla, J.D., (2008). Control of the timing of promoter escape and RNA catalysis by the transcription factor IIb fingertip. J. Biol. Chem., 283, 15665–15671.

[15] Čabart, P., Újvári, A., Pal, M., Luse, D.S., (2011). Transcription factor TFIIF is not required for initiation by RNA polymerase II, but it is essential to stabilize transcription factor TFIIB in early elongation complexes. *Proc. Natl. Acad. Sci. U. S. A.*, 108, 15786–15791.

- [16] Kugel, J.F., Goodrich, J.A., (1998). Promoter escape limits the rate of transcription from the adenovirus major late promoter on negatively supercoiled templates. *Proc. Natl. Acad. Sci. U. S. A.*, 95, 9232–9237.
- [17] Juven-Gershon, T., Cheng, S., Kadonaga, J.T., (2006). Rational design of a super core promoter that enhances gene expression. *Nat. Methods*, 3, 917–922.
- [18] Kamakaka, R.T., Tyree, C.M., Kadonaga, J.T., (1991). Accurate and efficient RNA polymerase II transcription with a soluble nuclear fraction derived from *Drosophila* embryos. *Proc. Natl. Acad. Sci. U. S. A.*, 88, 1024–1028.
- [19] Kadonaga, J.T., (1990). Assembly and disassembly of the Drosophila RNA polymerase II complex during transcription. J. Biol. Chem., 265, 2624–2631.
- [20] Horn, A.E., Kugel, J.F., Goodrich, J.A., (2016). Single molecule microscopy reveals mechanistic insight into RNA polymerase II preinitiation complex assembly and transcriptional activity. *Nucleic Acids Res.*, 44, 7132–7143.
- [21] Cole, N.B., (2013). Site-specific protein labeling with SNAPtags. Curr. Protoc. Protein Sci., 73, 30.1 Unit.
- [22] Pan, G., Greenblatt, J., (1994). Initiation of transcription by RNA polymerase II is limited by melting of the promoter DNA in the region immediately upstream of the initiation site. J. Biol. Chem., 269, 30101–30104.
- [23] Tantin, D., Carey, M., (1994). A heteroduplex template circumvents the energetic requirement for ATP during activated transcription by RNA polymerase II. J. Biol. Chem., 269, 17397–17400.
- [24] Gilman, B., Drullinger, L.F., Kugel, J.F., Goodrich, J.A., (2009). TATA-binding protein and transcription factor IIB induce transcript slipping during early transcription by RNA polymerase II. J. Biol. Chem., 284, 9093–9098.
- [25] Dvir, A., Conaway, R.C., Conaway, J.W., (1997). A role for TFIIH in controlling the activity of early RNA polymerase II elongation complexes. *Proc. Natl. Acad. Sci. U. S. A.*, 94, 9006–9010.
- [26] Holstege, F.C.P., van der Vliet, P.C., Timmers, H.T.M., (1996). Opening of an RNA polymerase II promoter occurs in two distinct steps and requires the basal transcription factors IIE and IIH. EMBO J., 15, 1666–1677.

[27] Čabart, P., Luse, D.S., (2012). Inactivated RNA polymerase II open complexes can be reactivated with TFIIE. J. Biol. Chem., 287, 961–967.

- [28] Treutlein, B., Muschielok, A., Andrecka, J., Jawhari, A., Buchen, C., Kostrewa, D., Hog, F., Cramer, P., et al., (2012). Dynamic architecture of a minimal RNA polymerase II open promoter complex. *Mol. Cell.* 46, 136–146.
- [29] Wang, Y., Fairley, J.A., Roberts, S.G., (2010). Phosphorylation of TFIIB links transcription initiation and termination. *Curr. Biol.*. **20**, *548–553*.
- [30] Kulbachinskiy, A., Mustaev, A., (2006). Region 3.2 of the sigma subunit contributes to the binding of the 3'-initiating nucleotide in the RNA polymerase active center and facilitates promoter clearance during initiation. J. Biol. Chem., 281, 18273–18276.
- [31] Vassylyev, D.G., Sekine, S., Laptenko, O., Lee, J., Vassylyeva, M.N., Borukhov, S., Yokoyama, S., (2002). Crystal structure of a bacterial RNA polymerase holoenzyme at 2.6 Å resolution. *Nature*, 417, 712–719.
- [32] Kugel, J.F., Goodrich, J.A., (2000). A kinetic model for the early steps of RNA synthesis by human RNA polymerase II. J. Biol. Chem., 275, 40483–40491.
- [33] Weaver, J.R., Kugel, J.F., Goodrich, J.A., (2005). The sequence at specific positions in the early transcribed region sets the rate of transcript synthesis by RNA polymerase II in vitro. J. Biol. Chem., 280, 39860–39869.
- [34] Dexl, S., Reichelt, R., Kraatz, K., Schulz, S., Grohmann, D., Bartlett, M., Thomm, M., (2018). Displacement of the transcription factor B reader domain during transcription initiation. *Nucleic Acids Res.*, 46, 10066–10081.
- [35] Pal, M., Ponticelli, A.S., Luse, D.S., (2005). The role of the transcription bubble and TFIIB in promoter clearance by RNA polymerase II. Mol. Cell, 19, 101–110.
- [36] Goodrich, J.A., Tjian, R., (1994). Transcription factors IIE and IIH and ATP hydrolysis direct promoter clearance by RNA polymerase II. Cell, 77, 145–156.
- [37] Ly, E., Goodrich, J.A., Kugel, J.F., (2019). Monitoring transcriptional activity by RNA polymerase II in vitro using single molecule co-localization. *Methods*, 159-160, 45–50.
- [38] Thomas, M.J., Platas, A.A., Hawley, D.K., (1998). Transcriptional fidelity and proofreading by RNA polymerase II. Cell, 93, 627–637.